Supplemental Material

Supplemental Table 1

Clinicopathological features of qRT-PCR cohort of exon 3 *CTNNB1*-mutant endometrial carcinomas.

Characteristics (n = 29)	**No Recurrence**	**Recurrence**
Histology	**n =**	**n =**
Endometrioid	17	10
Non-endometrioid	2	0
FIGO Stage	**n =**	**n =**
I	14	7
II	1	0
III	3	2
IV	0	1
Unknown	1	
Grade	**n =**	**n =**
G1	3	1
G2	14	7
G3	2	2
Lymphovascular Space Invasion (LVSI	**n =**	**n =**
Yes	5	5
No	14	3
Unknown		2

Supplemental Table 2

Antibodies

Antibody	Source	Company	Catalog #/Clone
Alexa Fluor 594 goat anti-mouse IgG		Invitrogen	#A21206
Alexa Fluor 594 goat anti-mouse IgG		Invitrogen	#A11032
β-catenin	Rabbit polyclonal	Cell Signaling	#8480/D10AB
CD73	Rabbit	Cell Signaling	# 13160/D7F9A
E-cadherin	Mouse monoclonal	BD Biosciences	#36/E-Cadherin
GAPDH	Rabbit polyclonal	Cell Signaling	# 3683/14C10
HRP-conjugated anti-mouse IgG		Cell Signaling	#7076
HRP-conjugated anti-rabbit IgG		Cell Signaling	#7074
Myc-tag (WB)	Rabbit polyclonal	Cell Signaling	#2278/ 71D10
Myc-tag (IF)	Mouse monoclonal	Cell Signaling	#2276/9B11
SP 1	Rabbit polyclonal	Cell Signaling	#9389/D4C3
Rab11a	Rabbit polyclonal	ABClonal	#A3251
H2AX	Rabbit polyclonal	Cell Signaling	#7631/D17A3
GSK3β	Rabbit monoclonal	Cell Signaling	#9312/27C10
pGSK3β S9	Rabbit polyclonal	Cell Signaling	#9323S/5B3
α-catenin	Rabbit monoclonal	Cell Signaling	#3240/23B2
GAPDH-HRP	Rabbit monoclonal	Cell Signaling	#3683S/14c10
SOX17	Rabbit polyclonal	ABclonal	#A18858
FOSL1	Rabbit polyclonal	ABclonal	#A5372

Supplemental Table 3

β-catenin target genes, downregulated in HEC-1-A *NT5E* KO cells

Gene	p-value, KO vs WT
GINS3	0.016997
SOX9	0.324417
UHRF1	0.043521
FOXRED2	0.056074
ABCC4	0.025321
SCARA3	0.037061
CCL28	0.00272
DKK1	0.011321
MNS1	0.002993
GINS2	0.05342
SLC7A2	0.015135
CLDN2	0.01134
SOX17	0.000201
MCM2	0.001181
ID2	0.000775
CCND1	0.002666
FAM111B	0.000191
RNF43	0.008008
ALDH1A1	0.000622
MMP7	0.006969

HDAC4	0.001222
EPHB3	0.002521
FZD7	0.000145

Supplemental Table 4

β-catenin target genes, upregulated in HEC-1-A *NT5E* KO cells

Gene	p-value, KO vs WT
ZNF367	0.147299
LGR5	0.101663
GJA1	0.24209
LOXL3	0.035689
PDK1	0.02015
CD3EAP	0.030654
PPARD	0.226127
NOS2	0.283438
SNAI1	0.016422
GBX2	0.040869
CD274	0.010798
TEAD4	0.063674
JUN	0.000082
PLAUR	0.005815
FOSL1	0.01345
DTL	0.005541
TFAP4	0.000273
FAM216A	0.000051
VEGFA	0.009235
CLDN1	0.001855
ANKRD13B	0.015263
GRAMD1A	0.002139
MYC	0.035353
JAG1	0.003937
CDT1	0.001499
FN1	0.100296
PALD1	0.018427
BAMBI	0.001473
NES	0.03024
STRA6	0.057879
TIAM1	0.061368

Supplemental Table 5

TCF-dependent Wnt target genes[1], downregulated in HEC-1-A *NT5E* KO cells

Gene	p-value, KO vs WT
TPI1P2	0.135108
NMNAT3	0.290828
PYGM	0.236633
MSX2	0.018796
SLC7A8	0.064381
HIST1H2BN	0.427417
BAG1	0.179839
HIST1H2AC	0.070826
HBP1	0.029965
CACNA1D	0.006801
BCL11B	0.021994
COL7A1	0.027357
TSHZ1	0.020746
THRB	0.00252
PAX2	0.011465
NEDD9	0.001869
B3GNT3	0.000015
CCND1	0.002666
DKK1	0.011321
CCDC87	0.028848
ELMO3	0.736051
LRIT3	0.649253
FERMT3	0.022604
SNAI3	0.008167

Supplemental Table 6

TCF-dependent Wnt target genes[1], upregulated in HEC-1-A *NT5E* KO cells

Gene	p-value, KO vs WT
GPR83	0.993146
UNC5C	0.186194
CYP2D7	0.780491
MYOM2	0.241658
EYA1	0.027181
CCNG2	0.024325
ZFAND2A	0.162111
PIP5KL1	0.079339
ANKRD24	0.020076
MSX1	0.014937
ANKRA2	0.000756
SYTL5	0.189944
HRH1	0.026711
THSD7A	0.405609
CCBE1	0.937148
KLLN	0.019551
PRPH	0.044281
GRM4	0.012582
MATN1-AS1	0.029069
HOXA9	0.130986
C1QL1	0.00512
JAK3	0.005432
TLL1	0.001282
RGS4	0.029391
SLC7A5P1	0.021268
INSC	0.000029
PLXNA2	0.03917
DDX60	0.114797
ADGRA2	0.090646
DOCK11	0.004414
PLAT	0.028507
RASSF6	0.008413
SYTL2	0.002717
CREBRF	0.008829
RASGEF1B	0.00022
NAP1L3	0.014844
SLC9A9	0.001679
TEX19	0.019683

RNF19B	0.007087
CLDN1	0.001855
ADAMTS5	0.005591
CALCB	0.012077
NTMT1	0.143381
ZNF503	0.000269
RPL41	0.152306
SOCS2-AS1	0.045362
SCUBE1	0.126216

Supplemental Table 7

Novogene-defined differentially expressed genes with D32N, G34R, and S37F in *NT5E* KO cells vs. EV *NT5E* WT cells.

Gene	Description	Mutant(s)	Δ, KO vs WT	Involvement in cancer	References
LINC01389	Antisense	S37F	down	upregulation is associated with gastric cancer; correlated with EMT	[2]
AC008438.1	Antisense	S37F	down	upregulation in some cancers	[3]
AL080317.1	Antisense	S37F G34R	down	upregulated in colon cancer; HR > 1 for Wilms tumor	[4,5]
AC092119.2	lincRNA	S37F D32N	down	upregulated in gastric cancer, ccRCC	[6]
LINC00113	lincRNA	S37F D32N	down	upregulated in TNBC, correlating with poor prognosis; up in lung cancer; downregulated in esophageal cancer; down in ccRCC	[7–10]
MIR3613	miRNA	S37F	down	down in CRC; tumor suppressor in breast cancer;	[11,12]
TUBA1A	protein_coding	S37F G34R	down	up in GC; up in GBM	[13,14]
HSPA1A	protein_coding	S37F G34R D32N	down	up in breast cancer; CRC	[15,16]
U2AF1	protein_coding	S37F D32N	down	Mixed/Unknown	[17,18]
ZNF112	protein_coding	S37F	down	Unknown	
AP001107.4	Antisense	G34R	down	down in CRC;	[19,20]
AC010331.1	Antisense	G34R	down	favorable prognostic factor in bladder cancer + breast cancer	[21,22]
U62317.2	Antisense	G34R D32N	down	down in bladder cancer; high levels correlate with high OS in basal-like breast cancer;	[23,24]
USP46-AS1	lincRNA	G34R	down	increased OS in ccRCC and glioma; decreased in HCC	[25,26]

AC127024.5	lincRNA	G34R	down	HR 0.3 in pancreatic cancer	27,28
AC005392.2	lincRNA	G34R	down	pro-angiogenic in CRC; poor OS in AML	29,30
AC124312.2	lincRNA	G34R	down	risk factor for bladder cancer;	31
AC005332.3	lincRNA	G34R D32N	down	HR 0.7 in pancreatic cancer; pro-EMT in HCC	32–34
MIR5587	miRNA	G34R	down	Unknown	
MIR6783	miRNA	G34R	down	Mixed/Unknown	35
AC131235.3	Antisense	D32N	down	shorter survival in CSC;	36
FP236383.1	lincRNA	D32N	down	Unknown	
MIR641	miRNA	D32N	down	prohibited prolif/met but promoted apoptosis in lung cancer; tumor suppressor in lung cancer and cervical cancer	37,38
MIR3682	miRNA	D32N	down	migration and stemness in HCC, through PI3K/β-catenin;	39
MIR3939	miRNA	D32N	down	associated with RT sensitivity in cervical cancer; associated with response to sunitinib in ccRCC;	40,41
HIST2H2AA4	protein_coding	D32N	down	associated with T2DM + pancreatic cancer; associated with hypothermic response in breast cancer	42,43
HIST2H2AA3	protein_coding	D32N	down	down in HCC; associated with T2DM + pancreatic cancer; associated w/ hypothermic response in breast cancer; up in brain mets in breast cancer	42–45
NUDT4B	protein_coding	D32N	down	does not cause CRC cell prolif; excluded from pan-cancer study due to similar expression in tumor vs normal tissue;	46,47
U2AF1L5	protein_coding	D32N	down	poor OS in NPC;	48
F8A3	protein_coding	D32N	down	lower OS in neuroblastoma;	49
HIST3H2BB	protein_coding	D32N	down	hypermethylated in lung cancer;	50
ETV7	protein_coding	D32N	down	oncogene and inta-inflammatory in breast cancer; promotes CRC; doxorubicin resistance in breast cancer; poor OS in bladder cancer	51–54
VPREB3	protein_coding	D32N	down	expressed on tumor cells with C-MYC translocations	55

Figure S1

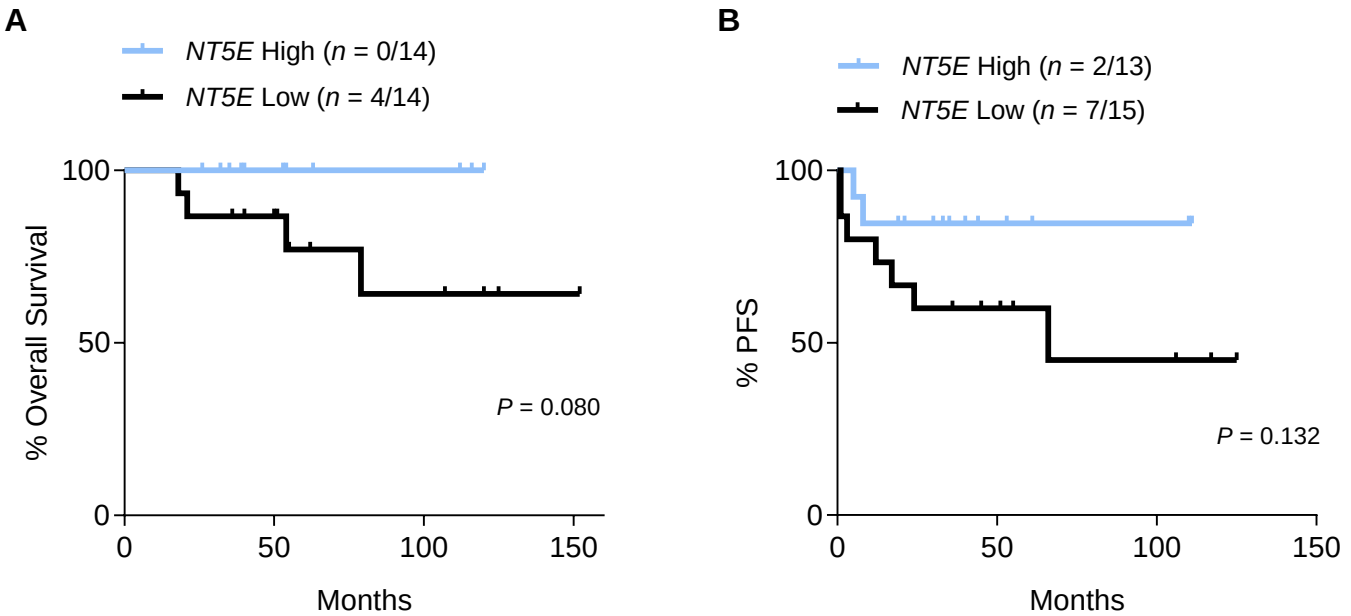
A
NT5E High (n = 0/14)
NT5E Low (n = 4/14)
% Overall Survival
100
50
0
P = 0.080
0
50
100
150
Months
B
NT5E High (n = 2/13)
NT5E Low (n = 7/15)
% PFS
100
50
0
P = 0.132
0
50
100
150
Months

Supplemental Figure Legends

Supplemental Figure 1. **Survival trends for patients with *NT5E* high and low exon 3 *CTNNB1* mutant tumors.** (**A**) Progression-free survival and (**B**) overall survival for patients with *NT5E* high and low endometrial tumors with exon 3 *CTNNB1* mutations. High and low values were determined by the median (0.001358). Logrank and Gehan-Breslow-Wilcoxon tests were used. *n* = 28 patients for (**A**) and (**B**), survival data was missing for one patient from the *n* = 29 cohort.

Figure S2

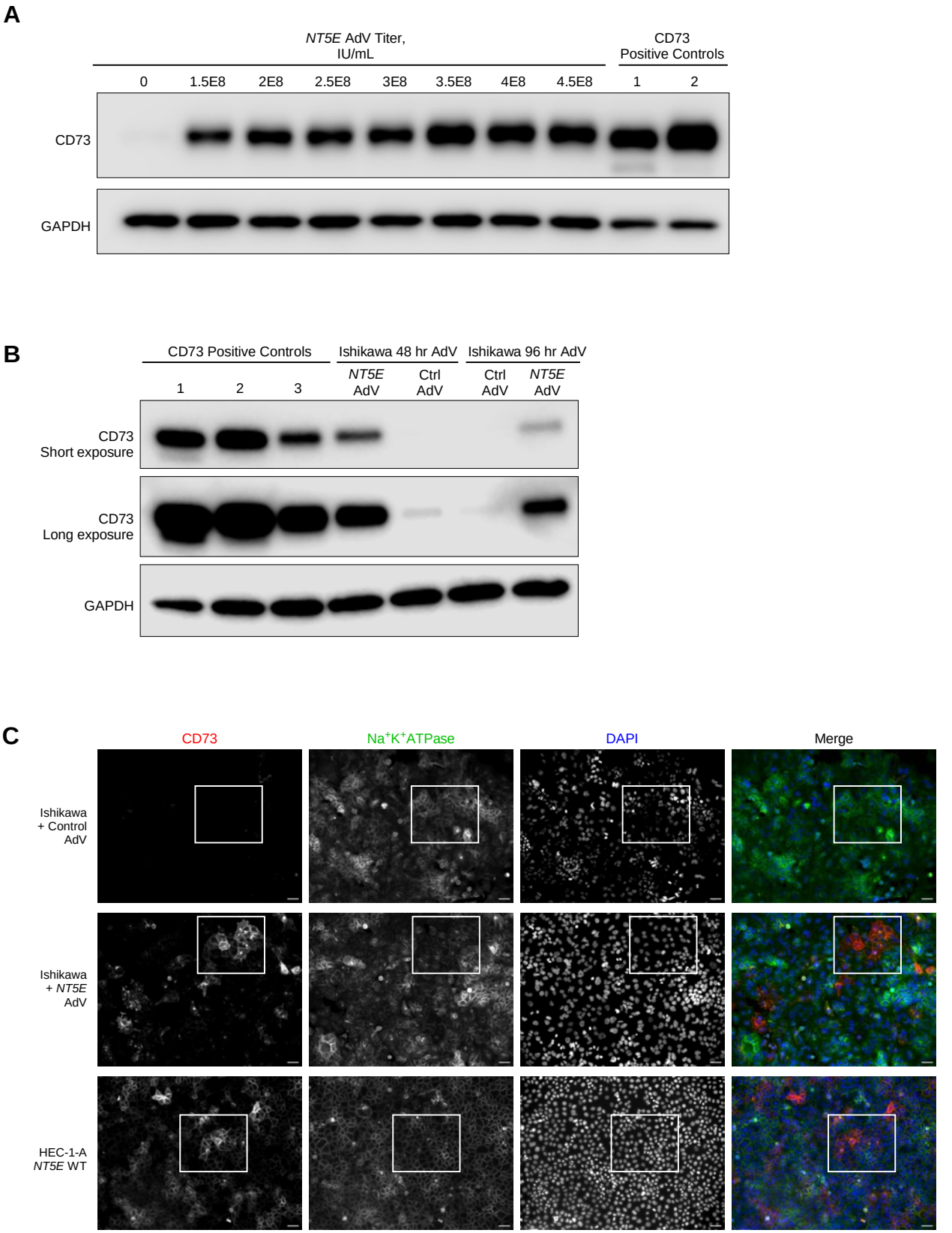
A
NT5E AdV Titer, IU/mL
CD73 Positive Controls
0
1.5E8
2E8
2.5E8
3E8
3.5E8
4E8
4.5E8
1
2
CD73
GAPDH
B
CD73 Positive Controls
Ishikawa 48 hr AdV
Ishikawa 96 hr AdV
1
2
3
NT5E AdV
Ctrl AdV
Ctrl AdV
NT5E AdV
CD73 Short exposure
CD73 Long exposure
GAPDH
C
CD73
Na+K+ATPase
DAPI
Merge
Ishikawa + Control AdV
Ishikawa + NT5E AdV
HEC-1-A NT5E WT

Supplemental Figure 2. Induced expression of CD73 via *NT5E* adenovirus transduction in Ishikawa cells. (**A**) CD73 protein expression with different *NT5E* AdV viral titers compared to HEC-1-A cells which serve as positive controls. CD73 Positive Control 1 = HEC-1-A cells at 100% confluency, 2 = HEC-1-A cells at 2 days post-confluency. (**B**) Validation of continued CD73 expression in Ishikawa cells. Expression persists for 96 hours, the endpoint in which TCF/LEF luciferase assays were performed. HEC-1-A cells serve as CD73 positive controls. Lanes 1 = HEC-1-A cells at 100% confluency; 2 = HEC-1-A cells at 2 days post-confluency; 3 = Ishikawa cells previously transduced with *NT5E* AdV and no luciferase reporter plasmids. NT = no transduction. (**C**) Uncropped immunofluorescence images corresponding to Fig. 2H. Cropped areas indicated with white rectangle. Scale bars 20 um.

Figure S3

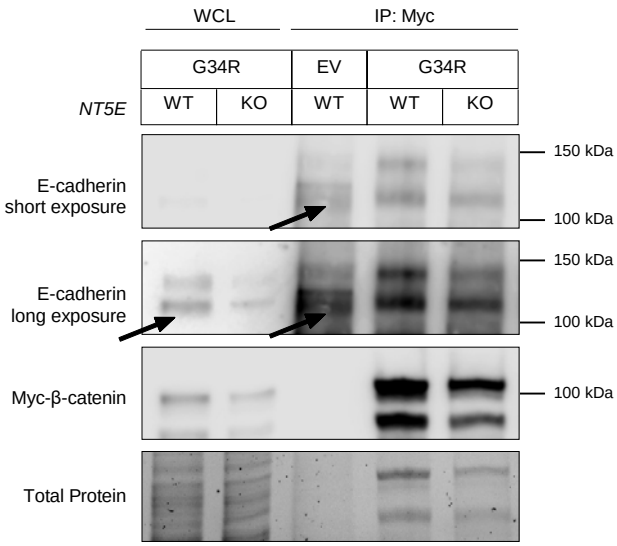
WCL
IP: Myc
G34R
EV
G34R
NT5E
WT
KO
WT
WT
KO
E-cadherin
short exposure
150 kDa
100 kDa
E-cadherin
long exposure
150 kDa
100 kDa
Myc-β-catenin
100 kDa
Total Protein

Supplemental Figure 3. Patient-specific exon 3 β-catenin mutant binds with E-cadherin. Immunoblots from co-immunoprecipitation experiment in *NT5E* WT and *NT5E* KO HEC-1-A cells. Myc-β-catenin was precipitated, and samples were probed for E-cadherin and myc-β-catenin expression G34R. *NT5E* KO cells have decreased expression of E-cadherin compared to *NT5E* WT cells. Thus, *NT5E* KO cells have a reduced capacity for E-cadherin-β-catenin binding. Accordingly, *NT5E* KO cells have weaker cell adhesions and increased nuclear β-catenin.

Figure S4

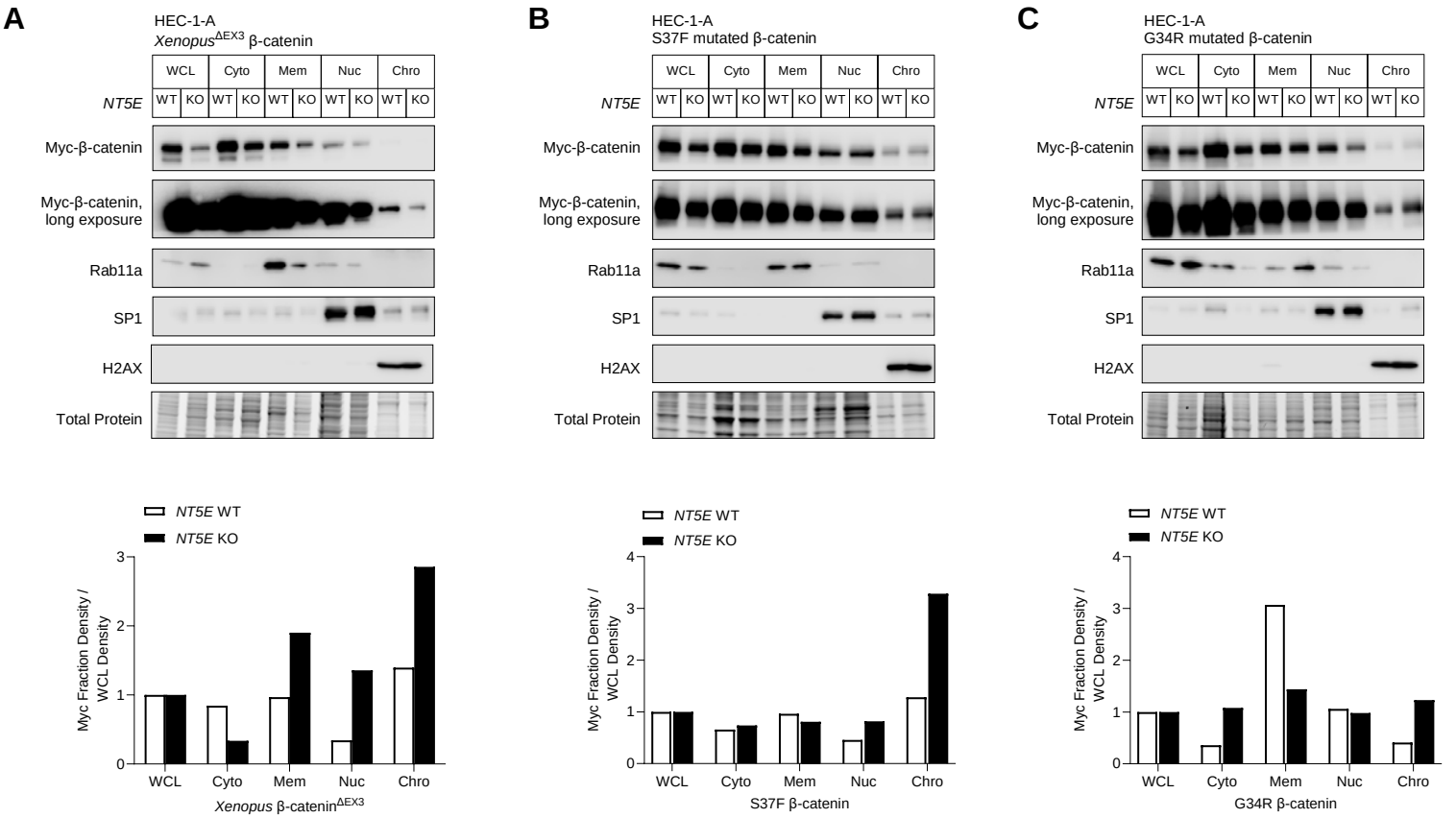
A
HEC-1-A
Xenopus ΔEX3 β-catenin
B
HEC-1-A
S37F mutated β-catenin
C
HEC-1-A
G34R mutated β-catenin
WCL
Cyto
Mem
Nuc
Chro
NT5E
WT
KO
Myc-β-catenin
Myc-β-catenin, long exposure
Rab11a
SP1
H2AX
Total Protein
NT5E WT
NT5E KO
Myc Fraction Density / WCL Density
Xenopus β-cateninΔEX3
S37F β-catenin
G34R β-catenin

Supplemental Figure 4. Independent replicates of cellular fractionations with patient-specific β-catenin mutations. (**A**, **B, C**) Independent replicates of the cellular fractionation experiments described in Fig. 4D, 4E, and 4F from *NT5E* WT and *NT5E* KO HEC-1-A cells. *NT5E* WT and *NT5E* KO HEC-1-A cells were transfected with patient-specific β-catenin mutants (**A**) *Xenopus* β-catenin$^{\Delta EX3}$, (**B**) S37F, or (**C**) G34R. Densitometry graphs are shown for myc-β-catenin mutant expression for each cellular fraction normalized to myc-β-catenin mutant expression in the whole cell lysate (WCL). Cellular fraction markers: Rab11a (membrane), SP1 (nuclear), and H2AX (chromatin).

Figure S5

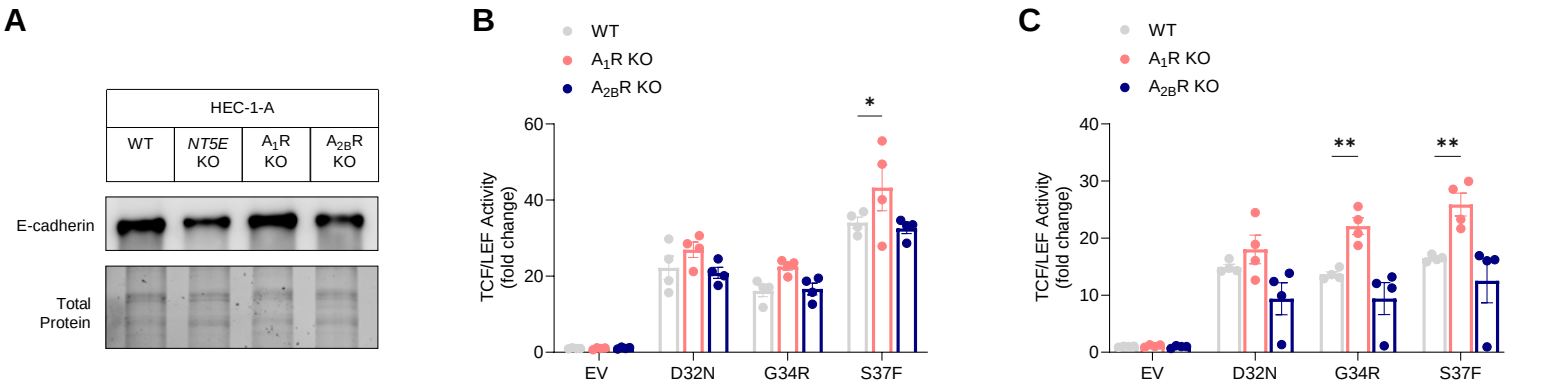
A
HEC-1-A
WT
NT5E KO
A1R KO
A2BR KO
E-cadherin
Total Protein
B
WT
A1R KO
A2BR KO
TCF/LEF Activity (fold change)
60
40
20
0
*
EV
D32N
G34R
S37F
C
WT
A1R KO
A2BR KO
TCF/LEF Activity (fold change)
40
30
20
10
0
**
**
EV
D32N
G34R
S37F

Supplemental Figure 5. Reduced transcriptional activity of patient-specific β-catenin mutants in A_1R KO cells. (**A**) Immunoblot showing E-cadherin expression is unchanged in HEC-1-A WT, *ADORA1* KO, and *ADORA2B* KO cells, but decreased in *NT5E* KO cells. (**B-C**) Independent replicates for data shown in Figure 6D. TCF/LEF reporter activity in cells transfected with empty vector (EV) or patient-specific β-catenin mutants D32N, G34R, or S37F. Each dot represents one technical replicate. Data represent mean ± SEM. *P < 0.05, **P < 0.01; 2-way ANOVA with Dunnett's post test.

Figure S6

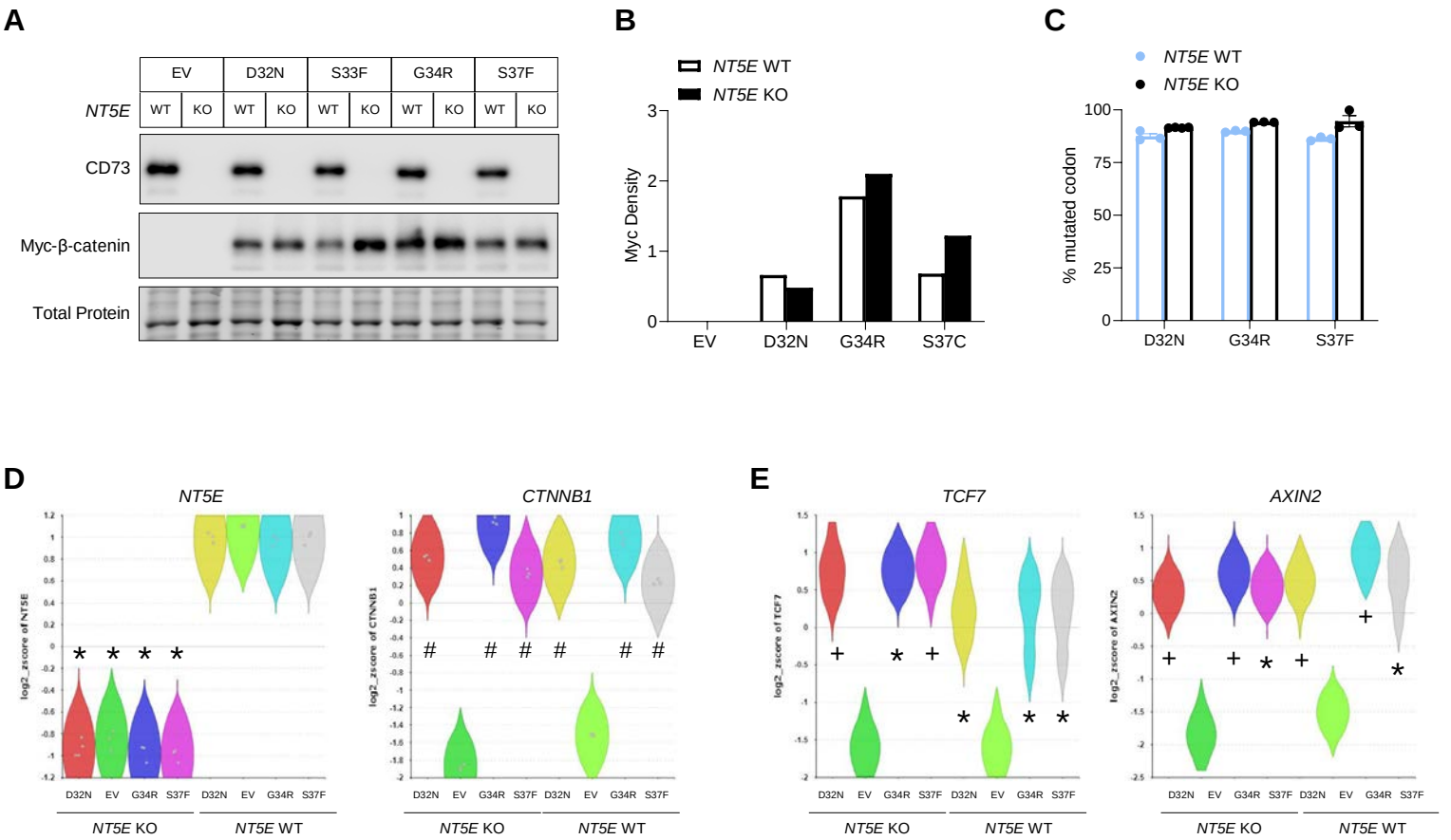

*P < 0.001 vs. *NT5E* WT
#P < 0.0005 vs EV

*P < 0.05 vs. EV
+P < 0.005 vs. EV

Supplemental Figure 6. Validation of patient-specific β-catenin mutant expression and activity in RNA-seq samples. (**A**) Protein samples were collected in sync with samples process and submitted for RNA-sequencing. Immunoblots were used to assess equal or near equal expression of each patient-specific β-catenin mutant between *NT5E* WT and *NT5E* KO HEC-1-A cells. Due to unequal protein expression of S33F between *NT5E* WT and *NT5E* KO samples, RNA from these samples was not submitted for sequencing. **(B**) Densitometry for myc-β-catenin from samples in (**A**) used for RNA-sequencing. (**C**) Mutation frequencies for D32N, G34R, and S37F, calculated using Integrative Genomics Viewer[56]. (**D-E**) Validation of our experimental system using mRNA expression levels from RNA-seq data. (**D**) As expected, NT*5E* levels were low in *NT5E* KO samples and *CTNNB1* expression increased in both *NT5E* KO and *NT5E* WT samples expressing patient-specific β-catenin mutants. (**E**) Validation of β-catenin mutants to induce Wnt/β-catenin signaling gene targets, *TCF7* and *AXIN2*, is shown.

Figure S7

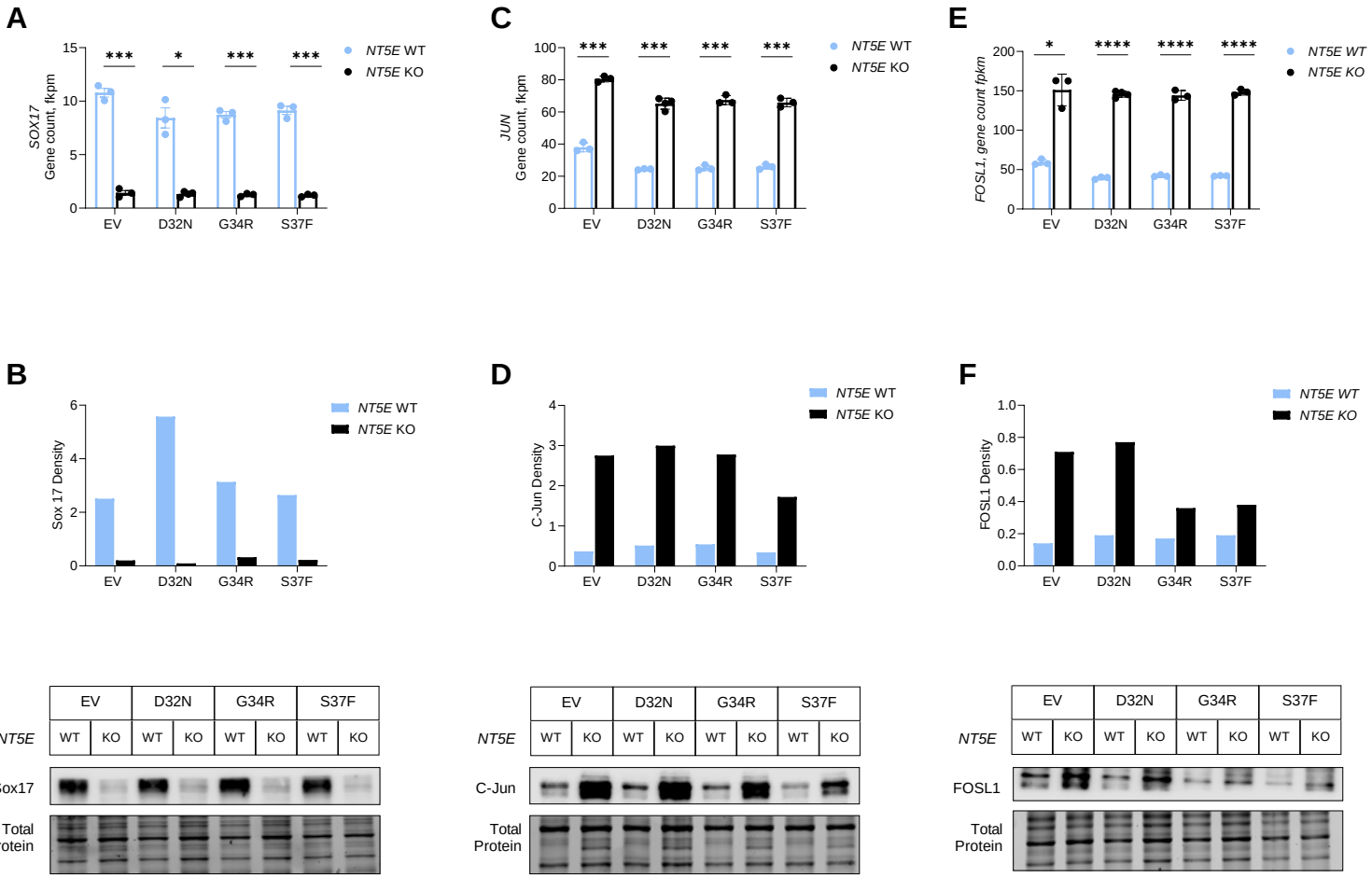
A
SOX17
Gene count, fkpm
15
10
5
0
***
*
***
***
EV
D32N
G34R
S37F
NT5E WT
NT5E KO
C
JUN
Gene count, fkpm
100
80
60
40
20
0
***
***
***
***
EV
D32N
G34R
S37F
NT5E WT
NT5E KO
E
FOSL1, gene count fpkm
200
150
100
50
0
*
****
****
****
EV
D32N
G34R
S37F
NT5E WT
NT5E KO
B
Sox 17 Density
6
4
2
0
EV
D32N
G34R
S37F
NT5E WT
NT5E KO
D
C-Jun Density
4
3
2
1
0
EV
D32N
G34R
S37F
NT5E WT
NT5E KO
F
FOSL1 Density
1.0
0.8
0.6
0.4
0.2
0.0
EV
D32N
G34R
S37F
NT5E WT
NT5E KO
EV
D32N
G34R
S37F
NT5E
WT
KO
Sox17
Total Protein
C-Jun
FOSL1

Supplemental Figure 7. Validation of dysregulated genes in *NT5E* WT and *NT5E* KO HEC-1-A cells identified from RNA-seq studies. (**A**) mRNA expression and (**B**) protein expression of Sox17 in *NT5E* WT and *NT5E* KO cells. (**C**) mRNA expression and (**D**) protein expression of C-Jun in *NT5E* WT and KO cells. (**E**) mRNA expression and (**F**) protein expression of Fra1 in *NT5E* WT and KO cells. (**B**, **D, F**) Representative immunoblots for $n = 3$ independent experiments. *P < 0.05, **P < 0.01, ***P < 0.005, Welch t-test.

Supplemental References

1. Doumpas, N., Lampart, F., Robinson, M.D., Lentini, A., Nestor, C.E., Cantù, C., and Basler, K. (2019). TCF/LEF dependent and independent transcriptional regulation of Wnt/β-catenin target genes. EMBO J. *38*, e98873. https://doi.org/10.15252/embj.201798873.

2. Taghehchian, N., Farshchian, M., Mahmoudian, R.A., Asoodeh, A., and Abbaszadegan, M.R. (2022). The expression of long non-coding RNA *LINC01389, LINC00365, RP11-138J23.1*, and *RP11-354K4.2* in gastric cancer and their impacts on EMT. Mol. Cell. Probes *66*, 101869. https://doi.org/10.1016/j.mcp.2022.101869.

3. Mitra, R., Adams, C.M., and Eischen, C.M. Systematic lncRNA mapping to genome-wide co-essential modules uncovers cancer dependency on uncharacterized lncRNAs. eLife *11*, e77357. https://doi.org/10.7554/eLife.77357.

4. Zeng, H., Xu, Y., Xu, S., Jin, L., Shen, Y., Rajan, K.C., Bhandari, A., and Xia, E. (2021). Construction and Analysis of a Colorectal Cancer Prognostic Model Based on N6-Methyladenosine-Related lncRNAs. Front. Cell Dev. Biol. *9*, 698388. https://doi.org/10.3389/fcell.2021.698388.

5. Liu, H., Zhang, M., Zhang, T., Shi, M., Lu, W., Yang, S., Cui, Q., and Li, Z. (2021). Identification of a ferroptosis-related lncRNA signature with prognosis for Wilms tumor. Transl. Pediatr. *10*, 2418–2431. https://doi.org/10.21037/tp-21-211.

6. Tang, C., Qu, G., Xu, Y., Yang, G., Wang, J., and Xiang, M. (2021). An immune-related lncRNA risk coefficient model to predict the outcomes in clear cell renal cell carcinoma. Aging *13*, 26046–26062. https://doi.org/10.18632/aging.203797.

7. Li, X., Jin, Y., Huang, J., Feng, C., Chen, X., Zuo, L., Liu, G., Chen, F., Fan, J., and Fang, L. (2024). Lnc00113 promotes triple-negative breast cancer progression via the NOB-1/MAPK signaling axis. J. Gene Med. *26*, e3662. https://doi.org/10.1002/jgm.3662.

8. Yang, Z., Li, H., Wang, Z., Yang, Y., Niu, J., Liu, Y., Sun, Z., and Yin, C. (2018). Microarray expression profile of long non-coding RNAs in human lung adenocarcinoma. Thorac. Cancer *9*, 1312–1322. https://doi.org/10.1111/1759-7714.12845.

9. Tian, Z.-H., Yuan, C., Yang, K., and Gao, X.-L. (2019). Systematic identification of key genes and pathways in clear cell renal cell carcinoma on bioinformatics analysis. Ann. Transl. Med. *7*, 89–89. https://doi.org/10.21037/atm.2019.01.18.

10. Li, C., Yao, W., Zhao, C., Yang, G., Wei, J., Qi, Y., Huang, R., Zhao, Q., and Hao, C. (2020). Comprehensive Analysis of lncRNAs Related to the Prognosis of Esophageal Cancer Based on ceRNA Network and Cox Regression Model. BioMed Res. Int. *2020*, 3075729. https://doi.org/10.1155/2020/3075729.

11. Gil-Kulik, P., Petniak, A., Kluz, N., Wallner, G., Skoczylas, T., Ciechański, A., and Kocki, J. (2023). Influence of Clinical Factors on miR-3613-3p Expression in Colorectal Cancer. Int. J. Mol. Sci. *24*, 14023. https://doi.org/10.3390/ijms241814023.

12. Chen, C., Pan, Y., Bai, L., Chen, H., Duan, Z., Si, Q., Zhu, R., Chuang, T.-H., and Luo, Y. (2021). MicroRNA-3613-3p functions as a tumor suppressor and represents a novel therapeutic target in breast cancer. Breast Cancer Res. BCR *23*, 12. https://doi.org/10.1186/s13058-021-01389-9.

13. Wang, D., Jiao, Z., Ji, Y., and Zhang, S. (2020). Elevated TUBA1A Might Indicate the Clinical Outcomes of Patients with Gastric Cancer, Being Associated with the Infiltration of Macrophages in the Tumor Immune Microenvironment. J. Gastrointestin. Liver Dis. *29*, 509–522. https://doi.org/10.15403/jgld-2834.

14. Wen, J., Wang, Q., Zhang, W., and Wang, W. (2023). TUBA1A licenses APC/C-mediated mitotic progression to drive glioblastoma growth by inhibiting PLK3. FEBS Lett. *597*, 3072–3086. https://doi.org/10.1002/1873-3468.14764.

15. de Freitas, G.B., Penteado, L., Miranda, M.M., Filassi, J.R., Baracat, E.C., and Linhares, I.M. (2022). The circulating 70 kDa heat shock protein (HSPA1A) level is a potential biomarker for breast carcinoma and its progression. Sci. Rep. *12*, 13012. https://doi.org/10.1038/s41598-022-17414-6.

16. Guan, Y., Zhu, X., Liang, J., Wei, M., Huang, S., and Pan, X. (2021). Upregulation of HSPA1A/HSPA1B/HSPA7 and Downregulation of HSPA9 Were Related to Poor Survival in Colon Cancer. Front. Oncol. *11*, 749673. https://doi.org/10.3389/fonc.2021.749673.

17. Palangat, M., Anastasakis, D.G., Fei, D.L., Lindblad, K.E., Bradley, R., Hourigan, C.S., Hafner, M., and Larson, D.R. (2019). The splicing factor U2AF1 contributes to cancer progression through a noncanonical role in translation regulation. Genes Dev. *33*, 482–497. https://doi.org/10.1101/gad.319590.118.

18. Zhu, Y., Song, D., Guo, J., Jin, J., Tao, Y., Zhang, Z., Xu, F., He, Q., Li, X., Chang, C., et al. (2021). U2AF1 mutation promotes tumorigenicity through facilitating autophagy flux mediated by FOXO3a activation in myelodysplastic syndromes. Cell Death Dis. *12*, 655. https://doi.org/10.1038/s41419-021-03573-3.

19. Chen, X., Zhang, Y., Chen, S., Yang, Y., Sun, G., and Pan, P. (2024). Construction of a nomogram for predicting HNSCC distant metastasis and identification of EIF5A as a hub gene. Sci. Rep. *14*, 13367. https://doi.org/10.1038/s41598-024-64197-z.

20. Chen, S., Li, X., Zhang, J., Li, L., Wang, X., Zhu, Y., Guo, L., and Wang, J. (2021). Six mutator-derived lncRNA signature of genome instability for predicting the clinical outcome of colon cancer. J. Gastrointest. Oncol. *12*, 2157–2171. https://doi.org/10.21037/jgo-21-494.

21. Wan, J., Guo, C., Fang, H., Xu, Z., Hu, Y., and Luo, Y. (2021). Autophagy-Related Long Non-coding RNA Is a Prognostic Indicator for Bladder Cancer. Front. Oncol. *11*, 647236. https://doi.org/10.3389/fonc.2021.647236.

22. Zhang, Y., Yue, Q., Cao, F., Li, Y., and Wei, Y. (2022). Necroptosis-related lncRNA signatures determine prognosis in breast cancer patients. Sci. Rep. *12*, 11268. https://doi.org/10.1038/s41598-022-15209-3.

23. Tan, W., Yuan, Y., Huang, H., Ma, J., Li, Y., Gou, Y., Wu, H., and Hu, Z. (2022). Comprehensive analysis of autophagy related long non-coding RNAs in prognosis, immunity, and treatment of muscular invasive bladder cancer. Sci. Rep. *12*, 11242. https://doi.org/10.1038/s41598-022-13952-1.

24. Cedro-Tanda, A., Ríos-Romero, M., Romero-Córdoba, S., Cisneros-Villanueva, M., Rebollar-Vega, R.G., Alfaro-Ruiz, L.A., Jiménez-Morales, S., Domínguez-Reyes, C., Villegas-Carlos, F., Tenorio-Torres, A., et al. (2020). A lncRNA landscape in breast cancer reveals a potential role for AC009283.1 in proliferation and apoptosis in HER2-enriched subtype. Sci. Rep. *10*, 13146. https://doi.org/10.1038/s41598-020-69905-z.

25. Klonisch, T., Logue, S.E., Hombach-Klonisch, S., and Vriend, J. (2023). DUBing Primary Tumors of the Central Nervous System: Regulatory Roles of Deubiquitinases. Biomolecules *13*, 1503. https://doi.org/10.3390/biom13101503.

26. An angiogenesis-related long noncoding RNA signature correlates with prognosis in patients with hepatocellular carcinoma (2021). Biosci. Rep. *41*. https://doi.org/10.1042/BSR20204442.

27. Hong, W.-F., Gu, Y.-J., Wang, N., Xia, J., Zhou, H.-Y., Zhan, K., Cheng, M.-X., and Cai, Y. (2021). Integrative Characterization of Immune-relevant Genes in Hepatocellular Carcinoma. J. Clin. Transl. Hepatol. *9*, 301–314. https://doi.org/10.14218/JCTH.2020.00132.

28. Wei, C., Liang, Q., Li, X., Li, H., Liu, Y., Huang, X., Chen, X., Guo, Y., and Li, J. (2019). Bioinformatics profiling utilized a nine immune-related long noncoding RNA signature as a prognostic target for pancreatic cancer. J. Cell. Biochem. *120*, 14916–14927. https://doi.org/10.1002/jcb.28754.

29. Huang, S., Wang, X., Zhu, Y., Wang, Y., Chen, J., and Zheng, H. (2023). SOX2 promotes vasculogenic mimicry by accelerating glycolysis via the lncRNA AC005392.2-GLUT1 axis in colorectal cancer. Cell Death Dis. *14*, 791. https://doi.org/10.1038/s41419-023-06274-1.

30. Yu, P., Lan, H., Song, X., and Pan, Z. (2020). High Expression of the SH3TC2-DT/SH3TC2 Gene Pair Associated With FLT3 Mutation and Poor Survival in Acute Myeloid Leukemia: An Integrated TCGA Analysis. Front. Oncol. *10*. https://doi.org/10.3389/fonc.2020.00829.

31. Ren, L., Yang, X., Liu, J., Wang, W., Liu, Z., Lin, Q., Huang, B., Pan, J., and Mao, X. (2023). An innovative model based on N7-methylguanosine-related lncRNAs for forecasting prognosis and tumor immune landscape in bladder cancer. Cancer Cell Int. *23*, 85. https://doi.org/10.1186/s12935-023-02933-7.

32. Tian, J., Fu, C., Zeng, X., Fan, X., and Wu, Y. (2022). An Independent Prognostic Model Based on Ten Autophagy-Related Long Noncoding RNAs in Pancreatic Cancer Patients. Genet. Res. *2022*, 3895396. https://doi.org/10.1155/2022/3895396.

33. Chen, G., Yang, G., Long, J., Yang, J., Qin, C., Luo, W., Qiu, J., Zhao, F., You, L., Zhang, T., et al. (2021). Comprehensive Analysis of Autophagy-Associated lncRNAs Reveal Potential Prognostic Prediction in Pancreatic Cancer. Front. Oncol. *11*, 596573. https://doi.org/10.3389/fonc.2021.596573.

34. Zhou, Y., Wang, L., Zhang, W., Ma, J., Zhang, Z., Yang, M., Yu, J., Luo, J., and Yan, Z. (2022). Identification of Epithelial Mesenchymal Transition-Related lncRNAs Associated with Prognosis and Tumor Immune Microenvironment of Hepatocellular Carcinoma. Dis. Markers *2022*, 6335155. https://doi.org/10.1155/2022/6335155.

35. Yao, Y., Hua, Q., and Zhou, Y. (2019). CircRNA has_circ_0006427 suppresses the progression of lung adenocarcinoma by regulating miR-6783–3p/DKK1 axis and inactivating Wnt/β-catenin signaling pathway. Biochem. Biophys. Res. Commun. *508*, 37–45. https://doi.org/10.1016/j.bbrc.2018.11.079.

36. Di, Z., Xu, G., Ding, Z., Li, C., Song, J., Huang, G., Zheng, J., Zhang, X., and Xiong, B. (2023). Identification and validation of a novel prognosis model based on m5C-related long non-coding RNAs in colorectal cancer. Cancer Cell Int. *23*, 196. https://doi.org/10.1186/s12935-023-03025-2.

37. Kong, Q., Shu, N., Li, J., and Xu, N. (2018). miR-641 Functions as a Tumor Suppressor by Targeting MDM2 in Human Lung Cancer. Oncol. Res. *26*, 735–741. https://doi.org/10.3727/096504017X15021536183490.

38. Zhu, Y., Liu, B., Zhang, P., Zhang, J., and Wang, L. (2019). LncRNA TUSC8 inhibits the invasion and migration of cervical cancer cells via miR-641/PTEN axis. Cell Biol. Int. *43*, 781–788. https://doi.org/10.1002/cbin.11152.

39. Zhang, Y., Cai, H., Wu, M.-H., Zhu, D.-H., Wang, X.-Y., Chen, Z.-Y., Yang, L., Liu, P., and Liu, Z. (2023). miR-3682-3p Activated by c-Myc Aggravates the Migration and Stemness in Hepatocellular Carcinoma Cells by Regulating PTEN/PI3K/AKT/β-Catenin Signaling. Dig. Dis. *41*, 447–457. https://doi.org/10.1159/000527800.

40. Tsaplina, N.N., Porkhanova, N.V., Fatkina, N.B., Zinkovich, M.S., Gusareva, M.A., Solntseva, A.A., Vasilieva, E.O., Kosheleva, N.G., Tolmacheva, E.A., Martynova, K.V., et al. (2022). From bioinformatic screening to low-invasive molecular diagnostics of the cervical tumor sensitivity to radiation therapy. J. Clin. Oncol. *40*, e17512–e17512. https://doi.org/10.1200/JCO.2022.40.16_suppl.e17512.

41. Zhang, H., Bai, L., Wu, X.-Q., Tian, X., Feng, J., Wu, X., Shi, G.-H., Pei, X., Lyu, J., Yang, G., et al. (2023). Proteogenomics of clear cell renal cell carcinoma response to tyrosine kinase inhibitor. Nat. Commun. *14*, 4274. https://doi.org/10.1038/s41467-023-39981-6.

42. Kasera, H., Shekhawat, R.S., Yadav, P., and Singh, P. (2023). Gene expression profiling and protein–protein network analysis revealed prognostic hub biomarkers linking cancer risk in type 2 diabetic patients. Sci. Rep. *13*, 22605. https://doi.org/10.1038/s41598-023-49715-9.

43. Amaya, C., Kurisetty, V., Stiles, J., Nyakeriga, A.M., Arumugam, A., Lakshmanaswamy, R., Botez, C.E., Mitchell, D.C., and Bryan, B.A. (2014). A genomics approach to identify susceptibilities of breast cancer cells to “fever-range” hyperthermia. BMC Cancer *14*, 81. https://doi.org/10.1186/1471-2407-14-81.

44. Khare, S.P., Sharma, A., Deodhar, K.K., and Gupta, S. (2011). Overexpression of histone variant H2A.1 and cellular transformation are related in N-nitrosodiethylamine-induced

sequential hepatocarcinogenesis. Exp. Biol. Med. Maywood NJ *236*, 30–35. https://doi.org/10.1258/ebm.2010.010140.

45. Mamoor, S. (2020). HIST2H2AA3 is differentially expressed in the lymph node and brain metastases of patients with metastatic breast cancer. Preprint at OSF, https://doi.org/10.31219/osf.io/sr769 https://doi.org/10.31219/osf.io/sr769.

46. Yan, S., Wang, Y., Gu, Y., Zhou, M., Su, L., Yin, T., Zhang, W., and Yue, Y. (2023). Baicalin suppresses colorectal cancer cell proliferation, potentially via ARRDC4: Bioinformatics and experimental analysis. Arab. J. Chem. *16*, 105141. https://doi.org/10.1016/j.arabjc.2023.105141.

47. He, C.-M., Zhang, X.-D., Zhu, S.-X., Zheng, J.-J., Wang, Y.-M., Wang, Q., Yin, H., Fu, Y.-J., Xue, S., Tang, J., et al. (2022). Integrative pan-cancer analysis and clinical characterization of the N7-methylguanosine (m7G) RNA modification regulators in human cancers. Front. Genet. *13*. https://doi.org/10.3389/fgene.2022.998147.

48. Zhao, S., Dong, X., Ni, X., Li, L., Lu, X., Zhang, K., and Gao, Y. (2021). Exploration of a Novel Prognostic Risk Signature and Its Effect on the Immune Response in Nasopharyngeal Carcinoma. Front. Oncol. *11*. https://doi.org/10.3389/fonc.2021.709931.

49. Zhang, P., Ma, K., Ke, X., Liu, L., Li, Y., Liu, Y., and Wang, Y. (2021). Development and Validation of a Five-RNA–Based Signature and Identification of Candidate Drugs for Neuroblastoma. Front. Genet. *12*. https://doi.org/10.3389/fgene.2021.685646.

50. Dong, S., Li, W., Wang, L., Hu, J., Song, Y., Zhang, B., Ren, X., Ji, S., Li, J., Xu, P., et al. (2019). Histone-Related Genes Are Hypermethylated in Lung Cancer and Hypermethylated HIST1H4F Could Serve as a Pan-Cancer Biomarker. Cancer Res. *79*, 6101–6112. https://doi.org/10.1158/0008-5472.CAN-19-1019.

51. Alessandrini, F., Pezzè, L., Menendez, D., Resnick, M.A., and Ciribilli, Y. (2018). ETV7-Mediated DNAJC15 Repression Leads to Doxorubicin Resistance in Breast Cancer Cells. Neoplasia *20*, 857–870. https://doi.org/10.1016/j.neo.2018.06.008.

52. Chai, B., Li, Y., Guo, Y., Zhang, Z., Jia, K., Chai, X., and Suo, Y. (2024). ETV7 promotes colorectal cancer progression through upregulation of IFIT3. Funct. Integr. Genomics *24*, 8. https://doi.org/10.1007/s10142-023-01282-y.

53. Li, H., Zhang, Y., and Zheng, S. (2021). Comprehensive Analysis Identified ETV7 as a Potential Prognostic Biomarker in Bladder Cancer. BioMed Res. Int. *2021*, 8530186. https://doi.org/10.1155/2021/8530186.

54. Meškytė, E.M., Pezzè, L., Bartolomei, L., Forcato, M., Bocci, I.A., Bertalot, G., Barbareschi, M., Oliveira-Ferrer, L., Bisio, A., Bicciato, S., et al. (2023). ETV7 reduces inflammatory responses in breast cancer cells by repressing the TNFR1/NF-κB axis. Cell Death Dis. *14*, 1–16. https://doi.org/10.1038/s41419-023-05718-y.

55. Rodig, S.J., Kutok, J.L., Paterson, J.C., Nitta, H., Zhang, W., Chapuy, B., Tumwine, L.K., Montes-Moreno, S., Agostinelli, C., Johnson, N.A., et al. (2010). The pre-B-cell receptor associated protein VpreB3 is a useful diagnostic marker for identifying c-MYC translocated

lymphomas. Haematologica *95*, 2056–2062.
https://doi.org/10.3324/haematol.2010.025767.

56. Robinson, J.T., Thorvaldsdóttir, H., Winckler, W., Guttman, M., Lander, E.S., Getz, G., and Mesirov, J.P. (2011). Integrative Genomics Viewer. Nat. Biotechnol. *29*, 24.
https://doi.org/10.1038/nbt.1754.